Asymmetrical competition between aquatic primary producers in a warmer and browner world

Francisco Rivera Vasconcelos,[2] Sebastian Diehl, Patricia Rodríguez,[1] Per Hedström, Jan Karlsson, and Pär Byström

Department of Ecology and Environmental Science, Umeå University, Umeå, Sweden

Abstract. In shallow lakes, pelagic and benthic producers engage in spatially asymmetrical resource competition. Pelagic producers intercept the flux of light to the benthic habitat and benthic producers intercept the flux of sediment-derived nutrients to the pelagic habitat. In boreal and subarctic regions, climate change is affecting this interaction both directly through warming and indirectly through increased loading with colored dissolved organic matter (cDOM) from the catchment ("brownification"). We use a dynamical ecosystem model to explore the consequences of these changing environmental conditions for lake primary production and compare model predictions with the results of an experiment in which we manipulated water temperature and cDOM supply in a 2 × 2 factorial design. The experiment was performed in field mesocosms large enough to harbor reproducing fish populations and was run over an entire growing season. In agreement with model predictions, benthic algal production and biomass declined and pelagic algal production and biomass increased with browning. Pelagic nutrient concentrations diverged over time between low and high cDOM treatments, suggesting that browning alleviated pelagic algal nutrient limitation by shading benthic competitors and preventing them from intercepting the release of nutrients from the sediment. Warming considerably reduced benthic and pelagic algal production as well as pelagic algal biomass and total phosphorus. The warming results are only in partial accordance with model expectations, but can be explained by an indirectly inferred, positive response of macrophyte production (which was not included in the model) to warming. Our study suggests that lake ecosystem responses to climate change are mediated by cross-habitat feedbacks between benthic and pelagic producers.

Key words: asymmetry; benthic; boreal; brownification; pelagic; resource competition; shallow lake; warming.

Introduction

Global warming affects ecosystems through a multitude of synergistic and antagonistic pathways. For example, at the level of primary producers, gross production rates (especially the light-dependent processes) tend to respond less strongly to warming than respiration rates and consumption rates by herbivores (Yvon-Durocher et al. 2010). Warming does, however, not only act directly on organisms but also indirectly through environmental feedbacks. For example, warming can affect aquatic systems through altered thermal stratification (Coma et al. 2009, Berger et al. 2010) or altered rainfall patterns and associated changes in material inputs from the terrestrial catchment (Dore 2005, Larsen et al. 2011). Thus, an understanding of complex feedbacks is required for the prediction of aquatic ecosystem responses to future climate change.

Small and shallow boreal lakes are the most abundant lake type in the world (Downing et al. 2006). They are

important in the global carbon cycle (Downing et al. 2006, Cole et al. 2007) and often strongly influenced by the surrounding terrestrial environment through the input of colored dissolved organic matter (cDOM; Williamson et al. 1999, Seekell et al. 2015a). The input of cDOM to boreal lakes has historically increased and is expected to further increase with changes in climate and atmospheric deposition (Monteith et al. 2007, Clark et al. 2010). Colored dissolved organic matter is a major driver of the light climate in nutrient-poor boreal lakes (Jones 1992, Williamson et al. 1999, Thrane et al. 2014). An increase of cDOM, therefore, contributes to the phenomenon of "brownification" (Kritzberg and Ekström 2012) and may lead to a shift of algal biomass and production from a prevalence of benthic producers in clear lakes to a prevalence of pelagic producers in colored lakes and an overall decrease in total primary production (Ask et al. 2009, Karlsson et al. 2009, Brothers et al. 2014). These cDOM effects have implications for secondary production up to fish in nutrient-poor boreal lakes (Karlsson et al. 2009, Finstad et al. 2013).

Competition between benthic and pelagic algae for the essential resources light and nutrients is asymmetrical in space, creating positive feedbacks of benthic and pelagic algae on themselves. Benthic algae inhabit the surface of

the relatively nutrient rich sediment and intercept sediment nutrients that could otherwise diffuse to their pelagic competitors; conversely, pelagic algae inhabit the relatively nutrient poor water column and attenuate light on the way to their benthic competitors (Hansson 1992). A recent dynamical model (Jäger and Diehl 2014) addressing these spatial asymmetries predicts that shallow and clear lakes should be dominated by benthic production and colored lakes by pelagic production, with a rather abrupt shift between the two states at some intermediate level of cDOM. Input of terrestrial cDOM is, in turn, often associated with higher (organic) nutrient input to the pelagic zone (Meili 1992), which should additionally favor the shift from benthic to pelagic production with increasing cDOM.

While considerable efforts have been devoted to the experimental study of the influence of warming on aquatic primary producers (e.g., Yvon-Durocher et al. 2010, Winder et al. 2012), very few studies have included cDOM loading as a treatment factor. Furthermore, the few available studies have been performed at small scales and have primarily focused on responses of pelagic algae (e.g., Graham and Vinebrooke 2009, Hansson et al. 2013; but see Mormul et al. 2012). Yet, experimental studies of climate change effects on small and shallow boreal lakes clearly need to address benthic producers and their interaction with pelagic producers. The latter requires a sufficiently large spatial scale such that cross-habitat interactions can become expressed without interference from cage artifacts such as epiphytic wall growth and shading from container walls.

Here we report on a field experiment exploring effects of multiple, climate-related, environmental changes on primary producers in shallow boreal waters. The study is unique in that it combines four features. First, we studied separate and interactive effects of warming and browning by manipulating water temperature and cDOM loading in a factorial design. Second, we documented the responses of both benthic and pelagic producers. Third, we performed the experiment at an unusually large spatial scale, using experimental units that minimized cage artifacts and harbored a complete food web including a reproducing population of invertebrate feeding fish. Finally, we combined the experiment with the extension and in-depth exploration of a process-based model of resource competition between benthic and pelagic producers, which provided testable predictions to compare with the experimental results. The major new insight emerging from this study is the proposition of a novel, positive feedback mechanism causing beneficial effects of cDOM on pelagic primary producers: shading by cDOM suppresses benthic algal production, which prevents benthic algae from intercepting the flux of limiting nutrients from the sediment to the pelagic habitat; the resulting increase in pelagic algal biomass further aggravates shading of the benthic habitat and reinforces the feedback loop.

MODEL STRUCTURE AND ANALYSES

Model description

The dynamical model has been described and analyzed in detail by Jäger and Diehl (2014). Here, we first briefly summarize its main assumptions and then extend it to include temperature dependence of several important process rates. The dynamical equations and the definitions, units, and numerical values of all parameters are listed in Tables 1 and 2.

The model assumes a highly simplified lake consisting of two habitats of uniform depth across the entire lake area, a well-mixed pelagic habitat that goes from the surface to the bottom of the water column at depth z_{max}, and a thin benthic habitat with thickness z_{bent} that reaches from the bottom of the mixed water column at z_{max} to the sediment surface at depth z_{sed}. The model describes the dynamics of six state variables: the carbon biomasses of pelagic (A) and benthic (B) algae, the concentrations of the limiting nutrient (assumed to be phosphorus) in the pelagic (R_{pel}) and benthic (R_{bent}) habitats, and light penetration to the bottom of the pelagic (I_{Zmax}) and benthic (I_{Zsed}) habitats.

Nutrients are supplied from two sources, the sediment with concentration R_{sed} and surface inflow with concentration R_{surf}. Nutrient exchange rates between the sediment and the benthic habitat and between the benthic and pelagic habitats are proportional to the concentration differences between habitats and the rate constants D_{bent}, and D_{pel}, respectively. Nutrient input from surface inflow occurs at the water exchange rate D_{surf}. Light attenuates with depth according to Lambert–Beer's law and is, at a given incoming light intensity I_0, fully described by the light intensities I_{Zmax} and I_{Zsed} at the bottom of the pelagic and benthic habitats, respectively. Light is attenuated by algal biomass (with attenuation coefficients k_A and k_B), and by background attenuation K_{bg} from, e.g., cDOM.

Pelagic and benthic algal production (P_A and P_B, respectively) depends on temperature T and is assumed to be colimited by light and the nutrient as described by two multiplicative saturation functions (Table 1: Eqs. T1.7 and T1.8). Growing algae take up mineral nutrients in proportion to algal production, assuming constant pelagic and benthic algal nutrient to carbon ratios c_A and c_B, respectively. Pelagic algae sink out of the water column at temperature-dependent velocity $v(T)$. Pelagic and benthic algae suffer from additional losses (from maintenance, grazing, viral lysis, etc.) at temperature-dependent rates $l_A(T)$ and $l_B(T)$, respectively. Pelagic algal losses are completely remineralized in the pelagic habitat, whereas only a fraction f_B of benthic algal losses is remineralized in the benthic habitat, the remainder being lost to the sediment. For simplicity, mineralization processes in the sediment are not explicitly modeled.

We modeled the temperature dependence of algal production, loss, and sinking rates using empirically estimated Q_{10} values derived from the literature

TABLE 1. Dynamical model with its differential and algebraic equations and the functions describing specific algal production.

Parameter	Equation	Eq. no.
Pelagic algal biomass (g C/m^3)	$\dfrac{dA}{dt} = \dfrac{A}{z_{\max}} \displaystyle\int_0^{z_{\max}} P_A(T, I(z), R_{pel}) dz - l_A(T)A - \dfrac{v(T)}{z_{\max}}A$	T1.1
Benthic algal biomass (g C/m^3)	$\dfrac{dB}{dt} = \dfrac{B}{z_{bent}} \displaystyle\int_{z_{\max}}^{z_{sed}} P_B(T, I(z), R_{bent}) dz - l_B(T)B$	T1.2
Dissolved pelagic nutrient concentration (g P/m^3)	$\dfrac{dR_{pel}}{dt} = \dfrac{D_{surf}}{z_{\max}}(R_{surf} - R_{pel}) + \dfrac{D_{pel}}{z_{\max}}(R_{bent} - R_{pel})$	T1.3
	$\quad + c_A l_A(T)A - \dfrac{c_A A}{z_{\max}} \displaystyle\int_0^{z_{\max}} P_A(T, I(z), R_{pel}) dz$	
Dissolved benthic nutrient concentration (g P/m^3)	$\dfrac{dR_{bent}}{dt} = \dfrac{D_{bent}}{z_{bent}}(R_{sed} - R_{bent}) - \dfrac{D_{pel}}{z_{bent}}(R_{bent} - R_{pel})$	T1.4
	$\quad + c_B f_B l_B(T)B - \dfrac{c_B B}{z_{bent}} \displaystyle\int_{z_{\max}}^{z_{sed}} P_B(T, I(z), R_{bent}) dz$	
Light intensity at depth $z_{\max}$ (μmol photons·m^{-2}·s^{-1})	$I_{z_{\max}} = I_0 e^{-(k_A A + K_{bg})z_{\max}}$	T1.5
Light intensity at depth z_{sed} (μmol photons·m^{-2}·s^{-1})	$I_{z_{sed}} = I_{z_{\max}} e^{-(k_B B + K_{bg})z_{bent}}$	T1.6
Specific production rate of pelagic algae (d^{-1})	$P_A(T, I(z), R_{pel}) = p_A(T)\dfrac{I(z)}{I(z) + h_A} \times \dfrac{R_{pel}}{R_{pel} + m_A}$	T1.7
Specific production rate of benthic algae (d^{-1})	$P_B(T, I(z), R_{bent}) = p_B(T)\dfrac{I(z)}{I(z) + h_B} \times \dfrac{R_{bent}}{R_{bent} + m_B}$	T1.8

Notes: Parameters are defined in Table 2. The dependence of parameters on temperature (T) is indicated and further specified in Table 3.

(Lopez-Urrutia et al. 2006, Englund et al. 2011, Bach et al. 2012; see Appendix S1 for a detailed description).

Model analyses

We performed extensive model simulations to explore the dynamical consequences of two major direct and indirect effects of global warming on boreal lakes: increased water temperature and increased input of terrestrial cDOM. Increased input of cDOM usually goes along with two correlated effects on resource supply (Meili 1992, Seekell et al. 2015b), which we varied independently in our simulations: (1) an increase in water color (described by background attenuation K_{bg}) and (2) an increase in dissolved nutrient supply to the water column (described by R_{surf}). We varied both parameters in 201 steps of 0.01 over the ranges 0.5–2.5/m (K_{bg}) and 0–0.5 g P/m^3 (R_{surf}), respectively. These values bracket the K_{bg} and R_{surf} ranges of our experimental treatments and of most boreal lakes with good margins. We limited our analyses of temperature effects to two temperature scenarios, ambient summer conditions (15°C) and warmed conditions (+5°C, corresponding to the upper bound of projected summer surface temperature increases in the Bothnian Sea at the end of the 21st century [Meier 2006]).

Most parameter values describing benthic and pelagic algal traits (at ambient temperature) were similar to those in Jäger and Diehl (2014), assuming that benthic algae have a higher biomass-specific light attenuation and nutrient content than pelagic algae and, consequently, are less competitive for nutrients but more competitive for light than pelagic algae (Table 2). Jäger and Diehl (2014) assumed, however, no nutrient recycling of benthic algal losses. Based on empirical data (e.g., Enoksson 1993) we set the remineralized fraction of benthic algal losses to 0.3, which yields realistic rates of epiphytic nutrient turnover (Mulholland et al. 1994, DeAngelis et al. 1995). This value is not critical. Qualitatively similar results are obtained when this fraction is varied between zero and 0.9. Where known, environmental parameters not varied in the simulations were set to their approximate values in the experimental system (D_{surf}, $z_{\max}$). We set R_{sed} to an empirically determined value representative of boreal-subarctic lakes in Sweden (F. Vasconcelos, *unpublished data*). Model simulations were run in GNU Octave 4.0 (Eaton et al. 2015) and in Matlab version R2013b (MathWorks, Natick, Massachusetts, USA), and we present results on algal biomass and production and pelagic nutrients at equilibrium.

MODEL PREDICTIONS

Effects of nutrient and light supply

Increasing inflow of surface nutrients (R_{surf}) and increasing water color (K_{bg}) are predicted to have

TABLE 2. Definitions, units, and numerical values of variables and parameters.

Variable/parameter	Value	Definition and units
A		biomass concentration of pelagic algae (g C/m^3)
B		biomass concentration of benthic algae (g C/m^3)
R_{bent}		concentration of dissolved nutrients in the benthic habitat (g P/m^3)
R_{pel}		concentration of dissolved nutrients in the pelagic habitat (g P/m^3)
c_A	0.008	phosphorus to carbon quota of pelagic algae (g P/g C)
c_B	0.015	phosphorus to carbon quota of benthic algae (g P/g C)
D_{bent}	0.05	nutrient exchange rate between sediment and benthic habitat (m/d)
D_{pel}	0.05	nutrient exchange rate between benthic and pelagic habitat (m/d)
D_{surf}	0.01	rate of external nutrient influx into pelagic habitat (m/d)
f_B	0.3	fraction of benthic algal losses that is mineralized in the benthic habitat (dimensionless)
h_A	80	half-saturation constant for light-limited production of pelagic algae (μmol photons·m^{-2}·s^{-1})
h_B	40	half-saturation constant for light-limited production of benthic algae (μmol photons·m^{-2}·s^{-1})
I_0	400	light intensity at the surface (μmol photons·m^{-2}·s^{-1})
k_A	0.0003	light attenuation coefficient of pelagic algae (m^2/mg C)
k_B	0.0005	light attenuation coefficient of benthic algae (m^2/mg C)
K_{bg}	0.5–2.5	background light attenuation coefficient (m^{-1})
l_A, l_B	ambient 0.1; warmed 0.145	loss rate of pelagic and benthic algae, respectively (d^{-1})
m_A	3	half-saturation constant for nutrient-limited production of pelagic algae (mg P/m^3)
m_B	5	half-saturation constant for nutrient-limited production of benthic algae (mg P/m^3)
p_A, p_B	ambient 1.5; warmed 1.831	maximum specific production rate of pelagic and benthic algae, respectively (d^{-1})
R_{sed}	0.03	concentration of dissolved nutrients in the sediment (g P/m^3)
R_{surf}	0–0.5	concentration of dissolved nutrients in surface influx (g P/m^3)
v	ambient 0.08; warmed 0.098	sinking velocity of pelagic algae (m/d)
z_{bent}	0.01	vertical extent of the benthic habitat (m)
z_{max}	1.6	depth of the pelagic habitat (below water surface; m)
z_{sed}	1.61	depth of the sediment surface (below water surface; m)

Note: Values of temperature sensitive parameters are shown for ambient (15°C) and warmed (20°C) conditions.

qualitatively very similar, negative effects on benthic algal production and biomass (Fig. 1a), because both lead to increased shading of the benthic habitat. The underlying mechanisms are, however, different: increasing water color shades the benthic habitat directly, whereas increasing nutrient inflow to the surface water benefits pelagic algae (Fig. 1b), which, in turn, shade the benthic habitat. Furthermore, the negative effects of both surface nutrients and water color on benthic algae are highly nonlinear as described next.

Starting from a clear, nutrient-poor system (low K_{bg} and R_{surf}, lower left corner in Fig. 1a), changes in benthic algal biomass with increasing surface nutrients and/or water color are initially small and gradual until a threshold is reached beyond which benthic algae decline rapidly to extinction (Fig. 1a, d). This is because, under baseline conditions (a shallow, clear system with a relatively low concentration of dissolved nutrients in the sediment), light supply is ample and both benthic and pelagic algal production are primarily nutrient limited. An increase in water color has, however, no effect on benthic algal nutrient supply, and neither does an increase in

surface nutrient supply, because the latter is almost completely converted into pelagic algal biomass (Fig. 1b). Instead, increasing water color and/or surface nutrients gradually decrease the light supply to the benthic habitat. This increases benthic light limitation and slowly but steadily decreases benthic algal production and biomass (Fig. 1a, d, g), thus weakening the interception of nutrients by benthic algae (Fig. 1c, f). Eventually, a threshold is reached beyond which a minor further increase in water color and/or surface nutrients leads to the rapidly accelerating decline of benthic algae to extinction (Fig. 1a, d). The underlying positive feedback works through the transport of sediment nutrients to the water column. Once benthic production becomes sufficiently strongly limited by light it can no longer intercept the greater part of the nutrient flow from the sediment to the water column. As a consequence, pelagic dissolved nutrients (Fig. 1c) and pelagic algal production (Fig. 1h) and biomass (Fig. 1b, e) increase steeply, further intensifying benthic algal light limitation (Fig. 1g) and, thus, further accelerating the flux of nutrients from the sediment to the water column.
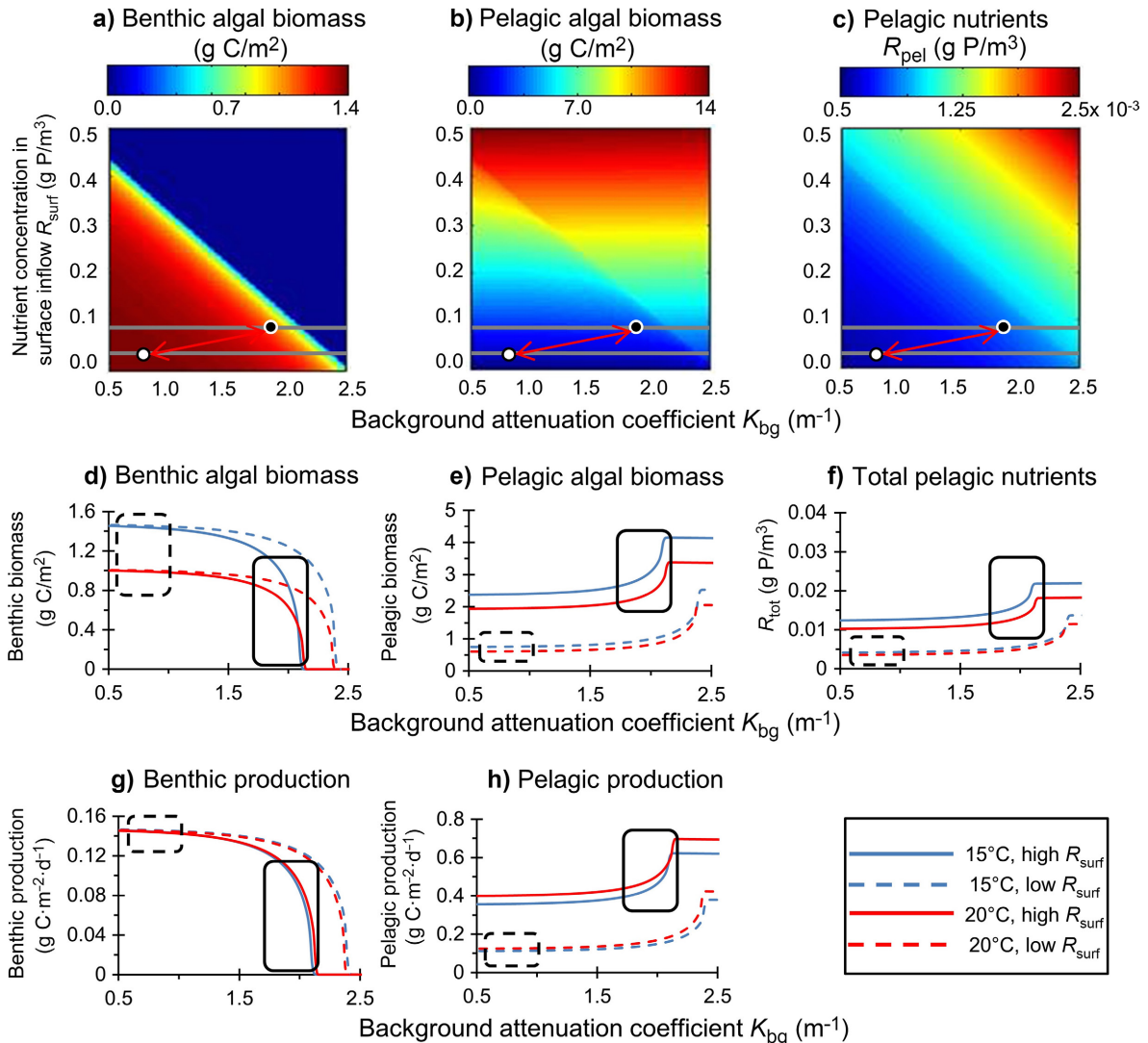
FIG. 1. Equilibrium predictions of the effects of background attenuation K_{bg} (assumed to be driven by colored dissolved organic matter [cDOM]), dissolved mineral nutrient concentration in the surface inflow R_{surf}, and warming on depth-integrated biomass and production of (a, d, g) benthic algae and (b, e, h) pelagic algae, (c) on dissolved mineral nutrient concentration in the water column R_{pel}, and (f) on total pelagic nutrient concentration R_{tot}. In the upper row of panels, dots connected by arrows indicate approximate conditions in the low (white dots) and high (black dots) cDOM treatments of the experiment. Panels d–h illustrate the influence of temperature on response variables along a gradient of background attenuation K_{bg} for two levels of nutrient concentration in the surface inflow R_{surf} (high, 0.095 g P/m^3; low, 0.030 g P/m^3), which are also shown as gray horizontal lines in panels a–c. All other parameters are as in Table 2. Broken and solid rectangles indicate approximate (qualitative) expectations for responses to the low cDOM (broken lines, low K_{bg}, low R_{surf}) and high cDOM (solid lines, high K_{bg}, high R_{surf}) treatments of the experiment.

Effects of temperature

Predicted effects of warming on benthic and pelagic production and biomass are similar along gradients of surface nutrients and water color. For clarity, we therefore illustrate them only along the water color dimension, but for two different levels of R_{surf} (Fig. 1d–h). At equilibrium, specific algal production and losses must balance. Because specific algal losses tend to increase more strongly with temperature than specific algal production (described by a higher Q_{10};

Table S1: Appendix S1), production and losses can only be in balance under warming if specific production is boosted by increased resource availability. Warming must therefore inevitably lead to a decrease in either benthic or pelagic equilibrium biomass or, most commonly, both (Fig. 1d, e), thus increasing resource availability through decreased (self-) shading and/or decreased interception of the nutrient flux from the sediment by benthic algae (both light levels and benthic and pelagic dissolved nutrient concentrations are typically higher under warming; data not shown).

Effects of warming on primary production are less straightforward to predict, because primary production is the product of two quantities that change in opposite directions with increasing temperature: (1) algal biomass, which is predicted to decrease with temperature (Fig. 1d, e; see previous paragraph), and (2) specific algal production, which is predicted to increase with temperature, because of direct temperature effects on specific production (Table S1: Appendix S1) and because of increased resource availability (see previous paragraph). For the model parameterization, in the numerical example, these two opposing trends cancel each other out with respect to the overall effect of temperature on benthic primary production (Fig. 1g), whereas for pelagic primary production the positive effects of temperature prevail (Fig. 1h).

EXPERIMENTAL METHODS

Study system and experimental design

To explore the separate and combined effects of warming and increased input of terrestrial cDOM on algal biomass, production, and resource levels, we experimentally manipulated water temperature and cDOM input in large outdoor mesocosms (Fig. 2) in a 2×2 factorial design with four replicates of each of the following treatments: ambient temperature and low cDOM input (subsequently called "ambient, low cDOM"); ambient temperature and high cDOM input ("ambient, high cDOM"); warming and low cDOM input ("warmed, low cDOM"); and warming and high cDOM input ("warmed, high cDOM"). The experiment was run from May to September 2012 (lasting 135 d) at the Umeå Experimental Ecosystem Facility (EXEF) near Umeå (63°48′ N, 20°14′ E). EXEF includes a pond (area 73×25 m) divided into 20 experimental units (subsequently called "sections") from which 16 were used for treatment establishment. Sections measured 12.5×7.3 m, had one 7.3 m long natural shoreline, and were separated by water-tight dark green PVC walls on the remaining sides. Each section was 1.6 m deep except for a narrow zone near the shoreline and had its own, separate water supply system.

The pond was filled with tap water from a ground water source in summer 2011. The high cDOM treatment was established beginning on 10 May 2012 (day 1) through the addition of humic water from a mid-sized stream near the facility. Initially, the water supply to both the high and low cDOM treatments was set to mimic a 2-week spring flow input of 4 m^3/d and thereafter a continuous input of 0.57 m^3/d, corresponding to a daily exchange rate of 0.4% of the water volume during the rest of the season. Humic stream water was 100-μm filtered prior to addition and was characterized by seasonal averages of 22.5 g/m^3 of dissolved organic carbon (DOC), 0.079 g/m^3 of total phosphorous (TP), and 0.662 g/m^3 of total nitrogen (TN). Tap water was
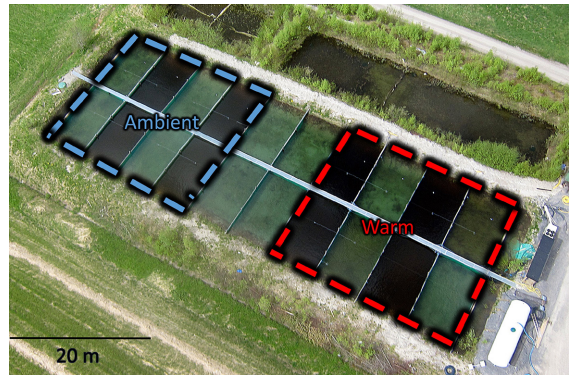

FIG. 2. Aerial photograph of the experimental facility (EXEF) showing the warmed and ambient temperature sections separated by buffer sections. Note that the low and high cDOM treatments can be easily distinguished visually. A container for the storage of high cDOM stream water and the shed harboring the heat exchanger are visible to the lower right.

characterized by seasonal averages of 1.6 g/m^3 DOC, 0.003 g/m^3 TP, and 0.071 g/m^3 TN. Treatments were blocked by temperature, the "ambient" and "warmed" treatments being separated by two buffer sections not used in this study (Fig. 2). Warming to 3°C above ambient water temperature was accomplished by continuously circulating water from the warmed sections through a heat exchanger.

Sections quickly developed natural pelagic and benthic communities, including sparse stands of floating leaf and submerged macrophytes. Sections were initially fishless, but were each stocked with 40 adult three-spined stickleback (*Gasterosteus aculeatus*) on 23 May (day 13). The fish subsequently reproduced during the season.

Physical, chemical and biological variables

Water temperature was recorded (loggers from Delta-T Devices, Cambridge, UK) every minute with sensors TH2-F from UMS (Munich, Germany) located at 0.5 m depth in the center of each section. We recorded vertical profiles of photosynthetically active radiation (PAR) in each section at 0.25 m depth intervals with a Li-250A radiometer equipped with a spherical quantum sensor Li-193SA (Li-Cor, Lincoln, Nebraska, USA) and calculated the vertical light attenuation coefficient k_d as the slope of a linear regression of the natural logarithm of PAR vs. depth (Kirk 2011). Assuming that vertical light attenuation followed Lambert–Beer's law, we calculated average light in the mixed water column as $100[1 - \exp(-k_d z)]/(k_d z)$ and light at the sediment surface as $100 \exp(-k_d z)$, both as percentages of incident PAR, where z is the depth of the water column. On four occasions we measured vertical temperature profiles. We did not detect any vertical temperature gradients on any of those occasions.

Every 3–4 weeks, we took integrated water samples from the upper 1 m of the water column, from which we

determined the concentrations of TP, TN, DOC, chlorophyll a (chl a), and particulate organic carbon (POC) as described in Appendix S1. TN is not further reported here because molar TN:TP ratios exceeded 30 throughout the experiment, indicating that P was the limiting nutrient for primary producers.

Because it is impossible to effectively and quantitatively separate benthic algae from soft sediment, we used artificial substrates to monitor benthic algal biomass. The substrates were made of cylindrical PVC pipe (height 3 cm, cross-sectional area 78.5 cm^2) that was open to the bottom (to allow for nutrient diffusion from below) and covered with a plankton net (mesh size 200 μm) for algal colonization. On three occasions (20 July, 20 August, 22 September) each section received three frames that were gently pushed into the sediment surface and allowed to develop a benthic algal biofilm. After three weeks, we sampled the frames by scraping all material from the plankton net into a container after invertebrates had been removed. The scraped material was suspended in 100 mL of Milli Q water (ELGA, High Wycombe, UK) from which we took subsamples of 5 mL for the subsequent determination of chl a and POC according to the protocols described in Appendix S1.

For comparison with model predictions algal biomass had to be expressed in units of carbon. We therefore converted measurements of chl a (which comes exclusively from living algae) to carbon using the relationship algal carbon biomass = measured chl a × POC:chl a ratio. Since the chl a content per unit of algal biomass can be sensitive to light and temperature (Cloern 1977, Baulch et al. 2009), we adjusted these estimates where necessary for treatment specific differences in the POC:chl a ratio (see Appendix S1 for details).

In order to assess potential differences in grazing pressure between treatments, we sampled zooplankton and zoobenthos at regular intervals. Zooplankton was sampled every three weeks by pulling a net (diameter 25 cm, mesh size 100 μm) from 1.3 m depth to the surface in the middle of each section. Samples were stored in Lugol's solution before analysis. Every six weeks, benthic invertebrates were sampled by pulling a 30 cm wide bottom net 70 cm along the sediment surface. Animals were stored in ethanol before analysis. Zooplankton and benthic animals were counted and measured digitally, and length–mass regressions were used to estimate biomass.

Primary production

Benthic and pelagic gross primary production (GPP) were estimated on two occasions (benthic, 6–10 August and 31 August–4 September; pelagic, 6–10 August and 28 September–1 October) from oxygen dynamics recorded during 48 h in situ incubations. Pelagic incubations were performed in cylindrical (height 0.32 m, volume 1.9 L) transparent acrylic containers suspended vertically 0.5–0.8 m below the water surface (one container per section). Over this 0.5–0.8 m depth range, the average

light was similar to the average light in the entire water column (0–1.6 m) to within ±5%. Benthic incubations were performed in semi-spherical (diameter 0.34 m, volume 12 L) transparent polycarbonate containers tightly grounded to the sediment surface (one container per section). Pelagic and benthic incubations were performed in eight sections at a time. Estimates of benthic GPP were not corrected for the contribution of phytoplankton from the enclosed water volume, because this contribution was generally low (Appendix S1). Whole-ecosystem GPP was inferred from oxygen dynamics recorded on two occasions (24–31 July and 14–21 September) using oxygen sensors deployed 0.5 m below the water surface in each section during one week. We also estimated GPP by submerged macrophytes (including epiphytes) as the difference between whole-ecosystem GPP and benthic plus pelagic production estimates. Further details of how changes in oxygen concentrations were converted to measures of carbon production are described in Appendix S1 and in Rodríguez et al. (2016).

Data analysis and statistics

For comparison of experimental data with model expectations, we calculated average values of all relevant state variables over the period day 100–135 (15 August–19 September). This time window was chosen because model predictions are for equilibrium conditions, which were most likely approached during late summer. Note that true equilibria were not expected in the experiment because environmental conditions (e.g., temperature and irradiation) were not constant over time. Since different state variables were not measured on exactly the same sampling dates, we calculated their average values across day 100–135 by linear interpolation between all available measurements during and immediately before and after the time window. Average values of ratios between two variables were calculated from log-transformed ratios.

Statistical significance of treatment effects on average values of state variables in the period day 100–135 was assessed with two-way ANOVA, where temperature (ambient vs. warmed) and cDOM loading (low vs. high) were the factors. Data were log-transformed ($\log(x)$) when necessary to fulfill ANOVA assumptions. All analyses were performed in R (R Development Core Team 2013).

Experimental Results and Comparison with Model Predictions

Treatment effectiveness and boundary conditions

The experimental warming and cDOM treatments were highly effective. Throughout the experiment, warmed sections were about 3°C warmer than ambient sections, whereas cDOM loading had no appreciable influence on water temperature (Fig. 3a, Table 3).
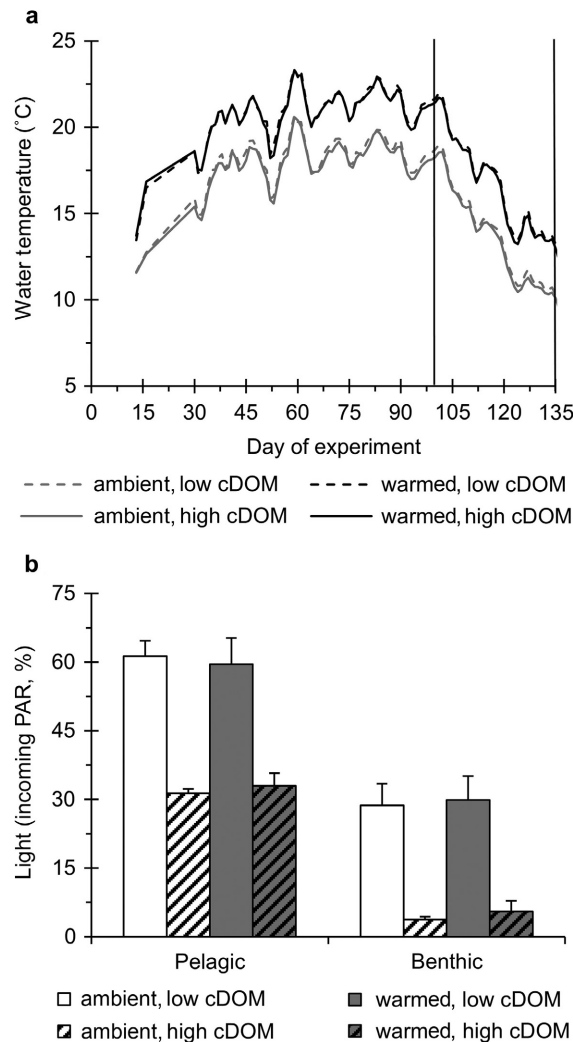
FIG. 3. Treatment effectiveness. (a) Water temperature over the course of the experiment. Values shown are means over the four replicates of each treatment. We report the measurements registered at noon (12:00) for each section. Vertical lines bracket the time window (day 100–135) over which all other response variables were averaged. (b) Average light in the mixed water column (pelagic) and light at the sediment surface (benthic), both as percentages of incoming photosynthetically active radiation (PAR). Values shown are treatment means and SE ($n = 4$) of measurements taken in the time window highlighted in panel a.

TABLE 3. *P* values from ANOVAs for the effects of the colored dissolved organic matter (cDOM) and temperature treatments and their interaction on benthic and pelagic light climate, total phosphorus, dissolved organic carbon (DOC), water temperature, the biomasses of zoobenthos and zooplankton, benthic and pelagic algal biomass, and the production of benthic and pelagic algae and macrophytes (including periphyton). Degrees of freedom are 1, 12 in all columns.

Variables	cDOM	Temperature	cDOM × Temperature
Light climate			
Benthic	<0.001*	0.69	0.93
Pelagic	<0.001*	0.98	0.64
Total phosphorus	0.025*	<0.001*	0.66
DOC	<0.001*	0.004*	0.30
Water temperature	0.069†	<0.001*	0.73
Zoobenthos	0.64	0.03*	0.38
Zooplankton	0.19	0.69	0.55
Benthic algal biomass	0.082†	0.31	0.53
Pelagic algal biomass	0.007*	0.019*	0.76
Benthic production	0.02*	<0.001*	0.17
Pelagic production	0.013*	<0.001*	0.10
Macrophyte + periphyton production	0.889	<0.05*	0.72

* $P < 0.05$; † $P < 0.1$.

In all treatments, total phosphorus concentrations increased from an average of 0.007 g P/m^3 on day 1 to approximately 0.02 g P/m^3 on day 42 (Fig. 4b), suggesting that sediment nutrients enriched the water column early in the season before a benthic algal layer had developed. Total phosphorus levels started to diverge between temperature treatments after day 42 and between cDOM treatments after day 100 (Fig. 4b; see also *Primary producers: linking experimental data and model predictions*). Zoobenthos and zooplankton did not differ significantly between cDOM treatments (Appendix S1: Fig. S2a, b; Table 3). Zooplankton did also not differ between temperature treatments, but zoobenthos was negatively affected by warming (Appendix S1: Fig. S2a, b; Table 3).

Primary producers: linking experimental data and model predictions

Benthic algal biomass and production were lower in high than in low cDOM sections, the effect on biomass being only marginally statistically significant (Table 3, Fig. 5a, d). In contrast, pelagic algal biomass and production, as well as total pelagic phosphorus concentration, were higher in high than in low cDOM sections (Table 3, Fig. 5b, c, e). These responses to the cDOM treatment are in almost complete qualitative agreement with model predictions (compare Figs. 5a–e with 1d–h).

Benthic and pelagic primary production, pelagic algal biomass, and pelagic phosphorus were all considerably lower in warmed than in ambient treatments, whereas benthic algal biomass showed no statistically significant

Conversely, light supply was unaffected by temperature treatment but was strongly reduced in the high cDOM treatment (Fig. 3b, Table 3). Specifically, average light in the mixed water column was 47% lower and light at the sediment surface was 84% lower in the high vs. low cDOM treatment (Fig. 3b). DOC concentration increased in all treatments during the first 60 d and then leveled off. During the focal period (day 100–135) DOC concentration was more than two times higher in the high vs. low cDOM treatments and was slightly lower in the warmed vs. ambient sections (Fig. 4a, Table 3).
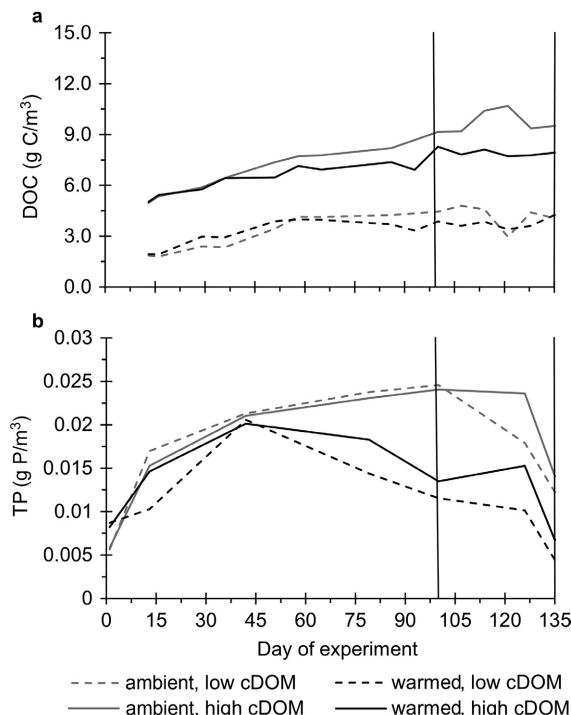
FIG. 4. Concentrations of (a) dissolved organic carbon (DOC) and (b) total phosphorus (TP) over the course of the experiment. Values shown are means over the four replicates of each treatment. Vertical lines bracket the time window (day 100–135) over which all other response variables were averaged.

response to warming (Fig. 5a–e, Table 3). While the responses of pelagic algal biomass and pelagic phosphorus to warming are in qualitative agreement with model expectations, the responses of benthic algal biomass and of algal production are not (compare Figs. 5a–e with 1d–h).

Our indirect estimates of macrophyte plus epiphyte production (which is not considered in the model) did not differ between the cDOM treatments, but were higher in warmed than in ambient treatments (Fig. 5f, Table 3).

DISCUSSION

Consistent with model expectations our experiment demonstrated negative effects of increased cDOM on benthic algal production and biomass and positive effects of increased cDOM on pelagic algal production and biomass as well as on pelagic TP. The experiment also showed clear negative effects of increased temperature on benthic and pelagic algal production and on pelagic biomass and TP, which are only partly consistent with model expectations. Here we discuss these results from both a theoretical and empirical perspective.

Effects of cDOM/brownification

The model predicts that increases in background attenuation K_{bg} (e.g., brownification) or in the nutrient

concentration in the surface inflow R_{surf} have very similar effects on the system. This is because dissolved nutrients from the surface inflow are close to proportionally converted into pelagic algal biomass (A), and incoming light to the benthic habitat decreases exponentially with the sum of biotic and abiotic light attenuation in the pelagic habitat ($k_A \times A + K_{bg}$; Table 1: Eq. T1.5). In our experiment, water color and the concentration of incoming surface nutrients could not be manipulated independently, because cDOM addition increased both light attenuation in the pelagic habitat and the total nutrient concentration in the incoming water. This is a realistic feature of our experiment, because cDOM carries both chromophores and organic nutrients in any natural system (Meili 1992, Larsen et al. 2011, Thrane et al. 2014). If organic nutrients carried by cDOM are equally available to producers as are mineral nutrients, we would then expect systems to move along a positively sloping trajectory in R_{surf}–K_{bg} space as cDOM concentration changes (shown by the double-headed arrows in Fig. 1a–c).

This raises the question to which extent increased pelagic biomass, production, and TP concentrations in the high cDOM treatments were a direct effect of organic nutrients added with cDOM vs. an indirect effect of increased nutrient release from the sediment caused by increased shading of benthic algae. A comparison of the time trajectories of DOC and TP concentrations gives surprisingly little support for the former mechanism. If organic nutrients added with cDOM were the main driver of the observed pelagic responses, one would expect to see a positive relationship between DOC and TP concentrations throughout the experiment. Instead, DOC and TP concentrations followed very different trajectories (Fig. 4a, b). DOC concentrations differed more than twofold between high and low cDOM treatments from the beginning to the end of the experiment. In contrast, TP concentrations were initially similar and increased synchronously in all treatments until day 42, indicating nutrient release from the sediment. TP concentrations subsequently diverged between temperature treatments, but not between cDOM treatments (day 42–100).

During the first 100 d of the experiment the huge difference in incoming TP concentration between high and low cDOM treatments (79 vs. 3 mg P/m³) was thus not at all reflected in pelagic TP concentrations. This suggests that nutrient fluxes across the benthic-pelagic boundary (e.g., sedimentation of seston, efflux of nutrients from sediment) must have swamped the signal from organic nutrients associated with cDOM. Together, these patterns indicate that organic nutrients associated with added cDOM were not readily available and that the mechanism predicted by our model, i.e., increased nutrient release from the sediment caused by increased shading of benthic algae by cDOM, contributed to the observed positive effects of cDOM on pelagic algae (see also Brothers et al. 2014). Only a few other studies have explored the influence of brownification on pelagic primary producers, and they
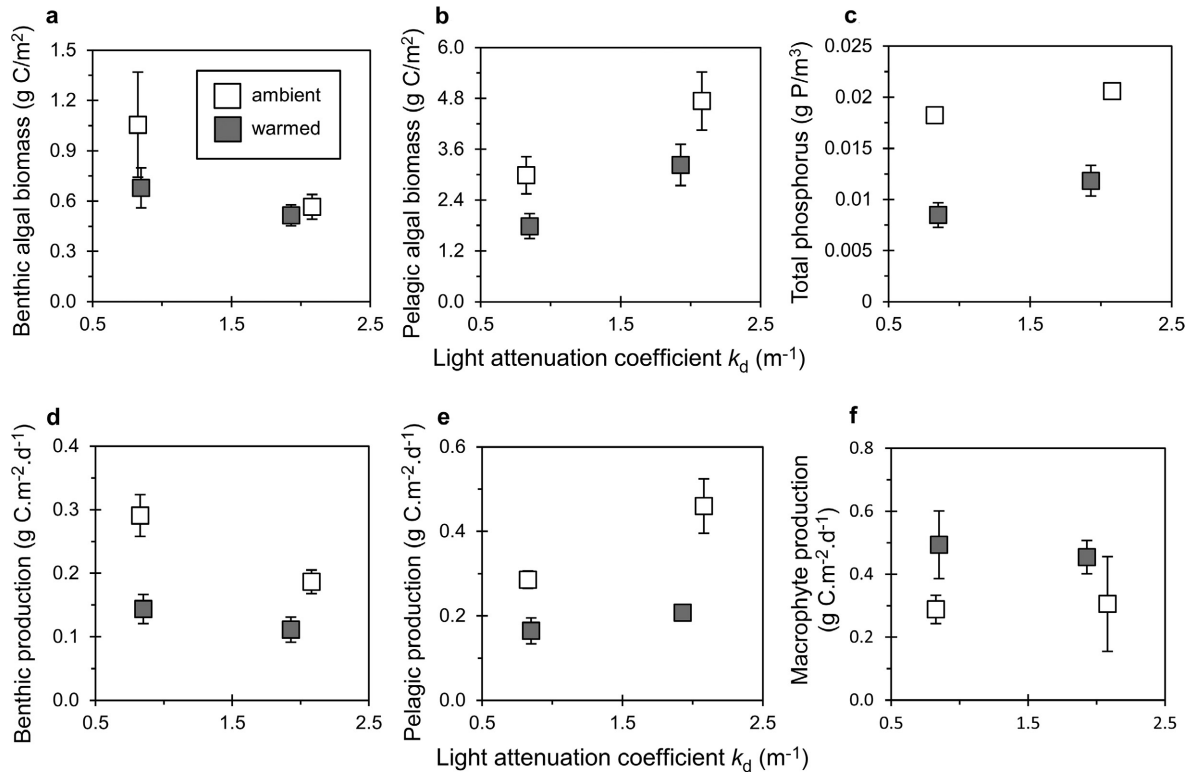
FIG. 5. Treatment responses: depth-integrated biomass of (a) benthic and (b) pelagic algae, (c) total pelagic phosphorus concentration, and depth-integrated production of (d) benthic and (e) pelagic algae and (f) of macrophytes (including periphyton). Values shown are treatment means ± SE ($n = 4$) of measurements taken in the time window day 100–135. In all panels, low cDOM treatments are on the left (measured photosynthetically active radiation [PAR] attenuation coefficient k_d 0.83–0.85) and high cDOM treatments on the right (k_d 1.93–2.08).

have typically also reported an increase of phytoplankton biomass or production in browner water (Ask et al. 2009, Mormul et al. 2012, Hansson et al. 2013, Brothers et al. 2014; but see Nicolle et al. 2012).

A distinctive feature of our model is that it predicts first a gentle, but eventually a very abrupt, decline of benthic algae beyond a threshold of either increasing background attenuation or increasing surface nutrient input (Fig. 1a). Near the threshold, a strong positive feedback of pelagic algae on themselves kicks in: pelagic algae shade out benthic algae sufficiently to increase the nutrient flux from the benthic to the pelagic habitat, which further enhances pelagic algal biomass, and so on. Note that this threshold depends not only on surface nutrient input and background attenuation but also on the depth of the water column over which light is attenuated. Our experiment was not designed to describe this benthic extinction threshold, but one could conceive an experiment in which the input of cDOM or mineral nutrients (or water column depth) is varied across a large gradient in order to characterize the threshold. Note, however, that complete extinction of benthic algae hinges on the (unrealistic) model assumption of a uniform water depth. In real lakes with more gently sloping shore topography, benthic algae have a competitive refuge on very shallow, well-lit bottoms and therefore cannot go completely extinct.

Effects of temperature

Our model predictions concerning temperature effects depend crucially on the assumption that rates of primary production are less temperature sensitive than metabolic and other loss rates, which is empirically well supported (Vázquez-Domínguez et al. 2007, Yvon-Durocher et al. 2010, 2012). The resulting predictions concerning the responses of algal biomass and resource levels to increased temperature are then straightforward, and we expect them to be qualitatively robust: if algal loss rates increase more rapidly with warming than do maximum production rates, specific algal production can only keep pace with these increased loss rates if resource availability increases. This, in turn, requires algal biomass to decrease with warming. The latter expectation was clearly borne out for pelagic algal biomass in both our study and other warming experiments (Feuchtmayr et al. 2009, Yvon-Durocher et al. 2010). In contrast, benthic algal biomass tended to respond negatively to warming only in the low but not in the high cDOM treatment (Fig. 5a). Note, however, that this observation would be consistent with expectations if we presume that high cDOM treatments came relatively close to the benthic extinction threshold, where benthic algal biomass is predicted to converge for all temperatures (compare Figs. 1d and 5a). Again, a

more elaborate experimental design (a broader and more finely spaced cDOM gradient cross-classified with different temperatures) would be required to test this model expectation more rigorously.

Compared to predictions of biomass responses, model predictions of temperature effects on primary production are more ambiguous, because they result from opposing direct (positive) effects of temperature on specific production and indirect (negative) effects on biomass. The exact outcome of a given increase in temperature will thus depend on the details of model parameterization. This said, it is nevertheless striking that the observed negative effects of warming on production were opposite in sign from the predicted ones. Moreover, while the model correctly predicted negative effects of warming on pelagic algal biomass and TP, the observed magnitude of these effects was considerably larger than predicted. We believe that these strong negative effects of warming were influenced by the presence of macrophytes in our experimental system. We indirectly estimated that the production of macrophytes (including epiphytes) was substantial and responded in opposite direction to temperature compared to benthic and pelagic algal production (Fig. 5d–f). While we did not measure macrophyte production and biomass directly, a positive response of macrophytes to warming over the temperature range encountered over the course of our experiment (10–23°C) is consistent with literature data (Barko et al. 1982, , Feuchtmayr et al. 2009, Landkildehus et al. 2014). Increased nutrient uptake by macrophytes may then have contributed to the rather strong reduction in pelagic TP and pelagic algal biomass in warmed treatments. To investigate this more rigorously, macrophytes should be included in the model; similarly, experiments should be performed in systems with and without macrophytes.

Interactions between warming and browning

We did not observe any interactive effects of the warming and browning treatments on any of the response variables. Note that this is a robust result, because we could experimentally separate effects of warming from effects of browning. In real lakes it is, however, likely that the two factors do not act independently from each other (Read and Rose 2013, Solomon et al. 2015). First, higher temperatures may speed up the degradation of DOM by microorganisms. We did indeed observe that DOC concentrations in the high cDOM treatment were lower at warm than ambient temperatures (Fig. 4a). Yet, this did not measurably affect the light environment (Fig. 3b), suggesting that colored components of the added DOM were not degraded faster at higher temperatures. Second, compared to clear lakes, humic lakes absorb solar radiation within a shallower surface layer and are typically warmer near the surface and colder at greater depths, and thus more steeply stratified (Solomon et al. 2015). In our experiment high cDOM treatments were not warmer than low cDOM treatments, which enabled us to

independently assess warming and cDOM effects. The absence of a temperature effect of cDOM was likely caused by the shallow nature of the experimental pond and the absence of thermal stratification. Radiation not directly absorbed by the water column was likely absorbed by surface sediment, from where it was transferred back as heat to the mixed water column. In deeper lakes, the influence of browning on the depth and steepness of thermal stratification may, however, have significant consequences for the nutrient supply to the pelagic habitat, because a steeper thermocline will hamper the transfer of nutrients from the hypolimnion to the photic surface layer.

Conclusions

Both our model and our experiment demonstrate that climate change can have important impacts on primary producers in shallow boreal lakes through both direct pathways (warming) and indirect pathways (brownification; see also Solomon et al. 2015). Overall, the model and the data suggest that browning benefits pelagic production and biomass and reduces benthic production and biomass. The data furthermore suggest that warming reduces both pelagic and benthic algal biomass and benefits macrophytes. The model predicts that feedbacks from shading by cDOM and/or pelagic algae on the release of sediment nutrients may cause non-linearities in the responses of producers to cDOM. While our experimental data suggest that such feedbacks are important in shallow boreal systems, the relevant processes need to be better characterized. In particular, future studies should quantify nutrient fluxes from the sediment and assess the availability of cDOM associated nutrients in order to sort out the relative importance of these nutrient sources to primary producers.

Literature Cited

Ask, J., J. Karlsson, L. Persson, P. Ask, P. Byström, and M. Jansson. 2009. Terrestrial organic matter and light penetration: effects on bacterial and primary production in lakes. Limnology and Oceanography 54:2034–2040.

Bach, L. T., U. Riebesell, S. Sett, S. Febin, P. Rzepka, and K. G. Schulz. 2012. An approach for particle sinking velocity measurements in the 3-400 μm size range and considerations on the effect of temperature on sinking rates. Marine Biology 159:1853–1864.

Barko, J. W., D. G. Hardin, and M. S. Matthews. 1982. Growth and morphology of submersed freshwater macrophytes in

relation to light and temperature. Canadian Journal of Botany 60:877–887.

Baulch, H. M., M. A. Turner, D. L. Findlay, R. D. Vinebrooke, and W. F. Donahue. 2009. Benthic algal biomass—measurement and errors. Canadian Journal of Fisheries and Aquatic Science 66:1989–2001.

Berger, S. A., S. Diehl, H. Stibor, G. Trommer, and M. Ruhenstroth. 2010. Water temperature and stratification depth independently shift cardinal events during plankton spring succession. Global Change Biology 16:1954–1965.

Brothers, S., J. Köhler, K. Attermeyer, H. P. Grossart, T. Mehner, N. Meyer, K. Scharnweber, and S. Hilt. 2014. A feedback loop links brownification and anoxia in a temperate, shallow lake. Limnology and Oceanography 59: 1388–1398.

Clark, J. M., S. H. Bottrell, C. D. Evans, D. T. Monteith, R. Bartlett, R. Rose, R. J. Newton, and P. J. Chapman. 2010. The importance of the relationship between scale and process in understanding long-term DOC dynamics. Science of the Total Environment 408:2768–2775.

Cloern, J. E. 1977. Effects of light intensity and temperature on *Cryptomonas ovata* (Cryptophyceae) growth and nutrient uptake rates. Journal of Phycology 13:389–395.

Cole, J. J., et al. 2007. Plumbing the global carbon cycle: integrating inland waters into the terrestrial carbon budget. Ecosystems 10:171–184.

Coma, R., M. Ribes, E. Serrano, E. Jiménez, J. Salat, and J. Pascual. 2009. Global warming-enhanced stratification and mass mortality events in the Mediterranean. Proceedings of National Academy of Sciences USA 106:6176–6181.

DeAngelis, D. L., M. Loreau, D. Neergaard, P. J. Mulholland, and E. R. Marzolf. 1995. Modelling nutrient-periphyton dynamics in streams: the importance of transient storage zones. Ecological Modelling 80:149–160.

Dore, M. 2005. Climate change and changes in global precipitation patterns: What do we know? Environment International 31:1167–1181.

Downing, J. A., et al. 2006. The global abundance and size distribution of lakes, ponds, and impoundments. Limnology and Oceanography 51:2388–2397.

Eaton, J., D. Bateman, S. Hauberg, and R. Wehbring. 2015. GNU octave version 4.0 manual: a high-level interactive language for numerical computations. http://www.gnu.org/software/octave/doc/interpreter/

Englund, G., G. Öhlund, C. L. Hein, and S. Diehl. 2011. Temperature dependence of the functional response. Ecology Letters 14:914–921.

Enoksson, V. 1993. Nutrient recycling by coastal sediments: effects of added algal material. Marine Ecology Progress Series 92:245–254.

Feuchtmayr, H., R. Moran, K. Hatton, L. Connor, T. Heyes, B. Moss, I. Harvey, and D. Atkinson. 2009. Global warming and eutrophication: effects on water chemistry and autotrophic communities in experimental hypertrophic shallow lake mesocosms. Journal of Applied Ecology 46:713–723.

Finstad, A. G., I. P. Helland, O. Ugedal, T. Hesthagen, D. O. Hessen, and J. Grover. 2013. Unimodal response of fish yield to dissolved organic carbon. Ecology Letters 17:36–43.

Graham, M. D., and R. D. Vinebrooke. 2009. Extreme weather events alter planktonic communities in boreal lakes. Limnology Oceanography 54:2481–2492.

Hansson, L. A. 1992. Factors regulating periphytic algal biomass. Limnology and Oceanography 37:322–328.

Hansson, L. A., A. Nicolle, W. Granéli, P. Hallgren, E. Kritzberg, A. Persson, J. Björk, P. A. Nilsson, and C. Brönmark. 2013. Food-chain length alters community responses to global change in aquatic systems. Nature Climate Change 3:228–233.

Jäger, C. G., and S. Diehl. 2014. Resource competition across habitat boundaries: asymmetric interactions between benthic and pelagic producers. Ecological Monographs 84: 287–302.

Jones, R. I. 1992. The influence of humic substances on lacustrine planktonic food chains. Hydrobiologia 229:73–91.

Karlsson, J., P. Byström, J. Ask, P. Ask, L. Persson, and M. Jansson. 2009. Light limitation of nutrient-poor lake ecosystems. Nature 460:506–509.

Kirk, J. T. O. 2011. Light and photosynthesis in aquatic ecosystems. Third edition. University Press, Cambridge, UK.

Kritzberg, E. S., and S. M. Ekström. 2012. Increasing iron concentrations in surface waters—a factor behind brownification? Biogeosciences 9:1465–1478.

Landkildehus, F., et al. 2014. Climate change effects on shallow lakes: design and preliminary results of a cross-European climate gradient mesocosm experiment. Estonian Journal of Ecology 63:71–89.

Larsen, S., T. Andersen, and D. O. Hessen. 2011. Climate change predicted to cause severe increase of organic carbon in lakes. Global Change Biology 17:1186–1192.

Lopez-Urrutia, Á., E. S. Martin, R. P. Harris, and X. Irigoien. 2006. Scaling the metabolic balance of the oceans. Proceedings of the National Academy of Sciences USA 103:8739–8744.

Meier, H. E. M. 2006. Baltic Sea climate in the late twenty-first century: a dynamical downscaling approach using two global models and two emission scenarios. Climate Dynamics 27:39–68.

Meili, M. 1992. Sources, concentrations and characteristics of organic matter in softwater lakes and streams of the Swedish forest region. Hydrobiologia 229:23–41.

Monteith, D. T., et al. 2007. Dissolved organic carbon trends resulting from changes in atmospheric deposition chemistry. Nature 450:537–540.

Mormul, R. P., J. Ahlgren, M. K. Ekvall, L. A. Hansson, and C. Brönmark. 2012. Water brownification may increase the invasibility of a submerged non-native macrophyte. Biological Invasions 14:2091–2099.

Mulholland, P. J., A. D. Steinman, E. R. Marzolf, D. R. Hart, and D. L. DeAngelis. 1994. Effect of periphyton biomass on hydraulic characteristics and nutrient cycling in streams. Oecologia 98:40–47.

Nicolle, A., P. Hallgren, J. von Einem, E. S. Kritzberg, W. Granéli, A. Persson, C. Brönmark, and L. A. Hansson. 2012. Predicted warming and browning affect timing and magnitude of plankton phenological events in lakes: a mesocosm study. Freshwater Biology 57:684–695.

R Development Core Team. 2013. R: a language and environment for statistical computing. R Foundation for Statistical Computing, Vienna, Austria. www.R-project.org

Read, J. S., and K. C. Rose. 2013. Physical responses of small temperate lakes to variation in dissolved organic carbon concentrations. Limnology and Oceanography 58:921–931.

Rodríguez, P., P. Byström, E. Geibrink, P. Hedström, F. R. Vasconcelos, and J. Karlsson. 2016. Do warming and humic river runoff alter the metabolic balance of lake ecosystems? Aquatic Sciences. http://dx.doi.org/10.1007/s00027-015-0463-y

Seekell, D. A., J. F. Lapierre, J. Ask, A. K. Bergström, A. Deininger, P. Rodríguez, and J. Karlsson. 2015a. The influence of dissolved organic carbon on primary production in northern lakes. Limnology and Oceanography 60: 1276–1285.

Seekell, D. A., J. F. Lapierre, and J. Karlsson. 2015b. Trade-offs between light and nutrient availability across gradients of dissolved organic carbon concentration in Swedish lakes: implications for patterns in primary production. Canadian Journal of Fisheries and Aquatic Sciences 72:1663–1671.

Solomon, C. T., et al. 2015. Ecosystem consequences of changing inputs of terrestrial dissolved organic matter to lakes: current knowledge and future challenges. Ecosystems 18: 376–389.

Thrane, J. E., D. O. Hessen, and T. Andersen. 2014. The absorption of light in lakes: negative impact of dissolved organic carbon on primary productivity. Ecosystems 17: 1040–1052.

Vázquez-Domínguez, E., D. Vaqué, and A. M. Gasol. 2007. Ocean warming enhances respiration and carbon demand of coastal microbial plankton. Global Change Biology 13:1 327–1334.

Williamson, C. E., D. P. Morris, M. Pace, and O. G. Olson. 1999. Dissolved organic carbon and nutrients as regulators of lake ecosystems: resurrection of a more integrated paradigm. Limnology Oceanography 44:795–803.

Winder, M., S. A. Berger, A. Lewandowska, N. Aberle, K. Lengfellner, U. Sommer, and S. Diehl. 2012. Spring phenological responses of marine and freshwater plankton to changing temperature and light conditions. Marine Biology 159:2491–2501.

Yvon-Durocher, G., J. I. Jones, M. Trimmer, G. Woodward, and J. M. Montoya. 2010. Warming alters the metabolic balance of ecosystems. Philosophical Transactions of the Royal Society B 365:2117–2126.

Yvon-Durocher, G., et al. 2012. Reconciling the temperature dependence of respirations across timescales and ecosystem type. Nature 487:472–476.

SUPPORTING INFORMATION

Additional supporting information may be found in the online version of this article at http://onlinelibrary.wiley.com/doi/10.1002/ecy.1487/suppinfo

Appendix A. Extended methods and auxiliary results

Model parameterization: estimation of Q10 values

We modeled the temperature dependence of algal production, loss and sinking rates based on empirically estimated Q_{10} values derived from the literature (Table A1) as

$X(T) = X_0 Q_{10}^{(T-T_0)/10}$, where $X(T)$ is the rate at temperature T and X_0 is the rate at reference temperature T_0. When Q_{10} was not explicitly given we calculated it from estimates

of activation energy E_a using the relationship $Q_{10} = \exp\left(\dfrac{-E_a \cdot 10}{kT_1 T_2}\right)$, where k is the

Boltzmann's constant, and T is absolute temperature in kelvin with T_1 corresponding to 10°C and T_2 to 20°C. These bounds are similar to the temperature range in our experiment (ca. 10-21°C).

Table A1. Q_{10} values (determined for the temperature range 10-20°C) used in the parameterization of specific algal production (p_A and p_B), specific algal loss rate (l_A and l_B) and sinking velocity of pelagic algae (v), and their literature sources.

| Parameter	Q_{10}	Calculation	Source
p_A, p_B	1.50	Based on an average activation energy of algal production of -0.29	Lopez-Urrutia *et al.* (2006)
l_A, l_B	2.13	Based on an average activation energy of maximum ingestion rate of consumers of -0.54	Englund *et al.* (2011)
v	1.44	Based on an average increase of 40% per 9°C	Bach *et al.* (2012)

Laboratory methods water chemistry

TP was determined according to Murphy and Riley (1962) after digestion with potassium persulfate. TN and DOC were analyzed on an IL 550 TOC-TN analyzer (Hach-Lange Company, USA). Water samples were filtered and acidified prior to DOC analysis. Water samples for Chl *a* and POC determination were filtered onto glass fiber filters (Whatman GF/F, GE Health Care, Chalfont St Giles, UK; POC filters had been precombusted and acid washed) which were dried and frozen for later analysis. Chl *a* was extracted in ethanol (Jespersen and Christoffersen 1987) and measured on a spectrofluorometer (Perkin Elmer, LS45). POC was determined by combusting the filters in a burner integrated into the IL 550 TOC-TN analyzer.

Estimation of algal carbon biomass from chlorophyll a

We estimated algal carbon biomass from measurements of Chl *a* (which comes exclusively from living algae) multiplied by the POC: Chl *a* ratio. These estimates were adjusted for systematic treatment differences in the Chl *a*:POC ratio (see Figure A1 and Table A2). Specifically, the pelagic Chl *a*:POC ratio was lower in warmed than in ambient treatments (0.003 vs. 0.004 µg/µg) and overall considerably lower than the benthic Chl *a*:POC ratios. The latter were higher in high than low cDOM treatments (0.009 vs. 0.006 µg/µg). We used these numbers to convert Chl *a* measurements from each replicate into estimates of algal carbon biomass using the relationship: algal carbon biomass = measured Chl *a* * treatment specific POC: Chl *a* ratio.

Figure A1. (**a**) Benthic and (**b**) pelagic chlorophyll *a* (Chl *a*), (**c**) benthic and (**d**) pelagic particulate organic carbon (POC), and the (**e**) benthic and (**f**) pelagic ratio of chlorophyll *a* : POC. Shown are treatment means (± SE, n = 4) of measurements taken in the time window day 100-135. In all panels low cDOM treatments are on the left (measured PAR attenuation coefficient k_d 0.83-0.85) and high cDOM treatments on the right (k_d 1.93-2.08).
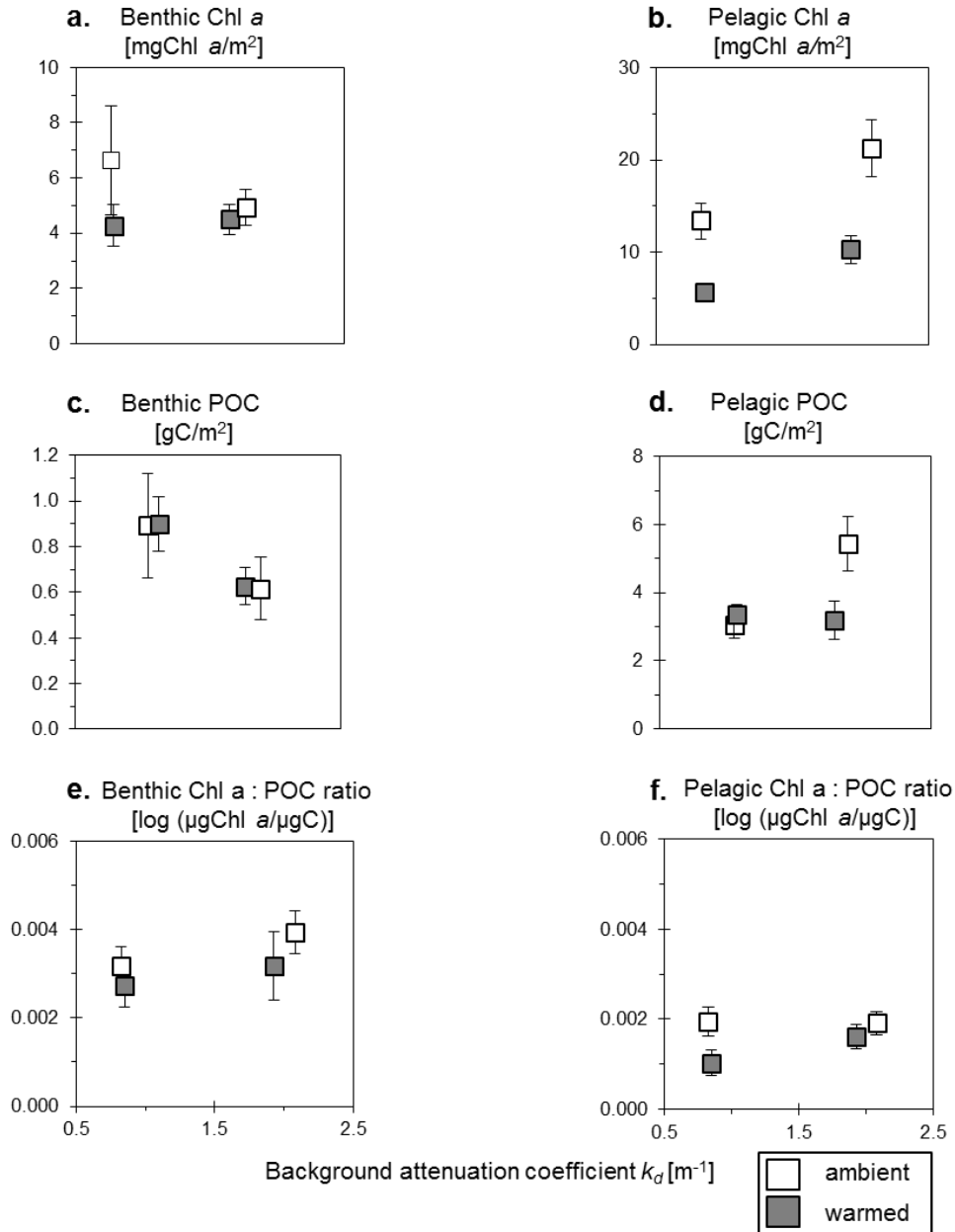
Table A2. Summary of ANOVAs of the effects of the cDOM and temperature treatments and their interaction on benthic and pelagic chlorophyll *a* (Chl *a*), benthic and pelagic particulate organic carbon (POC), and the benthic and pelagic chl *a* : POC ratio. Shown are degrees of freedom (1 treatment, 12 error degrees of freedom) and *P*-values. *P*-values < 0.05 are indicated by an asterisk and *P*-values < 0.1 by an asterisk in parentheses.

	Treatments, degrees of freedom and *P* values		
Variables	cDOM (1,12)	Temperature (1,12)	cDOM*Temperature (1,12)
Benthic Chl *a*	0.53	0.24	0.41
Pelagic Chl *a*	0.01 *	< 0.001 *	0.44
Benthic POC	0.09	0.96	0.99
Pelagic POC	0.13	0.16	0.042 *
Log Benthic Chl *a* : POC	0.052 (*)	0.24	0.35
Log Pelagic Chl *a* : POC	0.33	0.055 (*)	0.30

Estimation of benthic, pelagic and whole-ecosystem primary production from O_2 dynamics

Benthic, pelagic and whole-ecosystem GPP was inferred from the summed estimates of net community production and community respiration. Community respiration was calculated as the absolute value of the (negative) slope of O_2 concentration vs. time during nighttime, when GPP was assumed to be negligible. We also assumed that nighttime respiration equaled daytime respiration. Net community production was calculated as the slope of O_2 concentration vs. time during daytime when both primary production and respiration occurred. Finally, areal GPP (mg O_2 m^{-2} d^{-1}) was obtained as the sum of daytime net

community production and respiration, adjusted for the fraction of daylight hours per day and integrated over the depth of the water column.

Since benthic chambers contained pelagic water, phytoplankton contributed to an unknown extent to the oxygen dynamics in the benthic incubations. To assess to which extent estimates of GPP in benthic chambers could have been driven by phytoplankton, we conservatively assumed that phytoplankton in the benthic chambers had the same gross production as in the pelagic chambers. Thus estimated, phytoplankton contributed 8-10% to GPP in the benthic chambers in the low cDOM treatments and 15-20% in the high cDOM treatments. These already rather modest figures are likely substantial overestimates, because benthic chambers received considerably less light than the pelagic chambers (approximately 50% less in the low cDOM treatments and 80% less in the high cDOM treatments, Fig. 3b). Thus, since we had no reliable estimates of pelagic production near the bottom but knew that its contribution to oxygen dynamics in the benthic chambers was small, we did not correct our estimates of benthic GPP from the benthic chambers for the contribution from phytoplankton. Note that this is conservative with respect to the observed treatment responses. Since pelagic GPP responded positively to cDOM, correcting our estimates of benthic GPP for phytoplankton production (by subtracting the pelagic contribution to GPP from the observed GPP in the benthic chambers) should have accentuated the observed negative response of benthic GPP to cDOM.

Estimates of whole-ecosystem GPP were corrected for oxygen exchange with the atmosphere as described in Rodríguez *et al.* (2016). We also estimated GPP by submerged macrophytes (including epiphytes) as the difference between whole-ecosystem GPP and benthic plus pelagic production estimates. Estimates of total GPP were always greater than the sum of pelagic plus benthic GPP, except for one replicate where the subtraction was

slightly negative. All production estimates were converted to units of carbon assuming a $C:O_2$ conversion factor of 0.375 g/g (Wetzel and Likens 2000).

Results: biomass of zoobenthos and zooplankton

Figure A2. Biomass of (**a**) zoobenthos and (**b**) zooplankton. Shown are treatment means (± SE, n = 4) of measurements taken in the time window day 100-135. Low cDOM treatments are on the left (measured PAR attenuation coefficient k_d 0.83-0.85) and high cDOM treatments on the right (k_d 1.93-2.08).
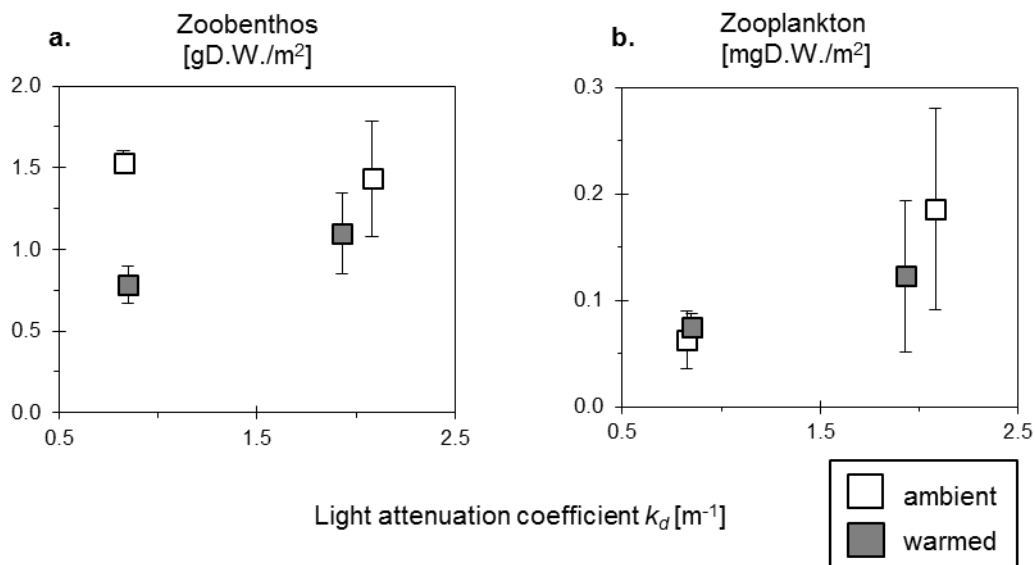
Cited references

Bach, L. T., U. Riebesell, S. Sett, S. Febin, P. Rzepka and K. G. Schulz. 2012. An approach for particle sinking velocity measurements in the 3-400 µm size range and considerations on the effect of temperature on sinking rates. Marine Biology 159: 1853-1864.

Englund, G., G. Öhlund, C. L. Hein and S. Diehl. 2011. Temperature dependence of the functional response. Ecology Letters 14: 914 – 921.

Jespersen, A. M. and K. Christoffersen. 1987. Measurements of chlorophyll-a from phytoplankton using ethanol as extraction solvent. Archiv fur Hydrobiologie 109: 445–454.

Lopez-Urrutia, Á., E. S. Martin, R. P. Harris and X. Irigoien. 2006. Scaling the metabolic balance of the oceans. Proceedings of the National Academy of Sciences 103: 8739-8744.

Murphy, J., and J. P. Riley. 1962. A modified single-solution method for the determination of phosphate in natural waters. Analytica Chimica Acta 27: 31–36.

Rodríguez, P., P. Byström, E. Geibrink, P. Hedström, F. R. Vasconcelos and J. Karlsson. 2016. Do warming and humic river runoff alter the metabolic balance of lake ecosystems? Aquatic Sciences DOI 10.1007/s00027-015-0463-y.

Wetzel, R. G. and G. Likens. 2000. Limnological Analyses. 3rd edition. Springer, New York.